VOL. 21, NO. 3, 2022, 62-68
https://elektrika.utm.my
ISSN 0128-4428

ELEKTRIKA
Journal of Electrical Engineering

Reduced-size Biocompatible Implantable Planar Inverted F- Antenna

Nuradilah Yusri, Raimi Dewan* and **Maheza Irna Mohamad Salim**

Advanced Diagnostics and Progressive Human Care, Department of Biomedical Engineering & Health Sciences, Faculty of Electrical Engineering, Universiti Teknologi Malaysia, UTM Johor Bahru, 81310 Johor, Malaysia

*Corresponding author: raimi.dar@utm.my

Abstract: The existence of implantable antennas presents intrinsic challenges as the performance of the antenna degrades due to the high losses of body tissues. In this study, a reduced-size Planar Inverted F- Antenna (PIFA) operating at Industrial, Scientific Medical (ISM) band (2.4 GHz) is designed and optimized. The design of PIFA is modeled to study and analyze the effect on the implantable antenna by placing it within the human body model, particularly in the arm. Copper is used as the patch material and the ground layer of the proposed antenna with Rogers RO3210 as its substrates. The simulation was carried within the human fat layer which is sandwich between the skin dan muscle layer. The design optimization of the antenna for operation in a human fat layer with optimal performance was achieved by reducing the size of the antenna. The antenna exhibits good stability with the reflection coefficient, S11 ≤ -10 dB at 2.4 GHz suitable for WBAN application in the environment of the human fat layer for near field communication. Analysis performance of the antenna was conducted by the transient movement of the antenna position due to the antenna being prone to movement when it is implanted within the body. The transient movement analysis is done when the implantable antenna is moving toward the skin layer and toward the muscle layer from the initial position within the fat layer. Additionally, 1 mm, 2 mm, interface of the layer and when the antenna within another tissue layer has been set to examine the performance of the implantable antenna. Correspondingly, simulation results indicate the impact of the human body layer due to the electrical properties of the human body in terms of conductivities, permittivity, and thicknesses of the layers. This has shown the design optimization of the antenna satisfies all requirements for an implantable antenna, such as small size of 5.08 × 4.00 × 0.66 (mm^3), biocompatible, low reflection coefficient of -42 dB at 2.4 GHz, realized gain of -18 dBi suitable for near field communication, and acceptable performance in fat layer. Future work will expand on conducting Specific Absorption Rate (SAR) to study the high attenuation of the radiated power of the human body on implanted antennas for the safety reason to bring in real life where it is being performed and examined.

Keywords: 2.4 GHz, Biocompatible, PIFA, Reduced size, Wireless

Article History: received 10 August 2022; accepted 30 October 2022; published 22 December 2022.

1. INTRODUCTION

Medical implants with the ability to communicate with an external device via wireless technology are known as implantable medical devices (IMDs). The usage of IMDs has increased in recent years because of the advantages provided in detecting and treating a variety of medical diseases in a wide spectrum of patients by giving real-time biotelemetric data [1]. These devices allow for the remote measurement of physiological signals using wired or wireless connection technologies. Electronic implantable medical devices (IMDs) are designed to be entirely or partially placed in human bodies through procedures and to stay in the body for several hours to many years, or even permanently for instance, after the surgical intervention. Wireless Body Area Networks (WBANs) are an intelligent network integration that allows devices and sensors to work together to collect a variety of key physiological parameters [2].

Implant WBANs for biomedical applications have recently undergone a paradigm shift because of advancements in antenna technology and wireless communication networks [3]. Implantable antenna plays an important role in medical healthcare toward increasing the quality of healthcare diagnosis, treatment, and medical research [4]. Implantable antennas can help to reduce the risk of some disease complications that may lead to chronic disease. Implantable antennas are electrically compact antennas that radiate into a lossy medium which is the human body tissues that influences the design of an effective implantable antenna. Previous research has demonstrated that antennas can operate optimally in open space however, when an antenna structure is implanted in the human body, the performance degrades, particularly in terms of frequency detuning, gain, radiation efficiency and radiation pattern [1].Thus, optimizing return loss, increasing antenna bandwidth, maintaining minimal size, ensuring patient safety, and achieving acceptable radiation performance are the fundamental design issue in developing an implanted antenna with satisfactory performances.

The existence of implantable antennas in biomedical telemetry represents an intrinsic challenge due to

performance of the implantable antenna in the human body layer degrades as the presence of lossy human body tissues [5][6]. that will affect the return loss, gain, radiation efficiency and radiation pattern. This problem has been widely addressed by the previous researchers on the implantable antenna for biomedical telemetry [9]. However, through this project it is expected to design a reduced size of biocompatible implantable antenna inside the human body model which is specifically inside the fat layer at the arm part. In this project, Planar Inverted F-Antenna (PIFA) is used for the simulation, and the standard frequency range follows the Industrial Scientific and Medical (ISM) band in which the antenna will be operated at 2.4 GHz.

2. METHODOLOGY

2.1 Tools and Software

Planar Inverted F- Antenna is the proposed type of the antenna that was designed, simulated, and optimized to obtain the optimal performance of the antenna inside the human body which is the arm part. CST Microwave Studio Software (student version) was used to model and simulate the structure of the antenna. Other than that, it is also used to analyze the parametric performance of the antenna when it is moving towards the skin and towards the muscle in proximity to the human body with a varying permittivity and thickness for body layers. Sigma Plot was used to plot the graph from results data that have been obtained from the CST Software.

The human body layer has different electrical properties such as permittivity (ε_r), conductivity (σ) and thickness are required to simulate the real environment for testing purposes. Human body model is made up of 3 main layers and the electrical properties of different tissues of the human body are varied depending on their types such as skin, fat, and muscle [4].

2.2 Design Stages of Proposed Antenna

A reduced size of Planar Inverted F-Antenna (PIFA) operates at ISM band is designed in this paper for implantable medical applications. The proposed antenna is designed by using a three-layer geometry model which consists of ground, substrate, and patch. The antenna is designed by using the substrate material, Rogers RO3210 which is a biocompatible material.

2.2.1 ***Stage A***

Design A is the design of the antenna in the free space. The length of the substrate is *SUBX*= 10 mm, and the width of the substrate is *SUBY*= 6.03 mm in the initial design of the antenna. The thickness of the ground plane and the radiating patch are *ANTt*=0.035 mm, *GNDTt*=0.035 mm respectively and the patch thickness is *SUBt*=0.59 mm.

The illustration depicts the surface view of the proposed antenna together with its geometrical specifications as shown in Figure 1 and Figure 2. The dimensions and values of the planned antenna are displayed in Table 1.

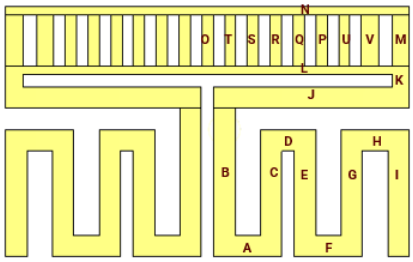

Figure 1. Design of the antenna in CST top view

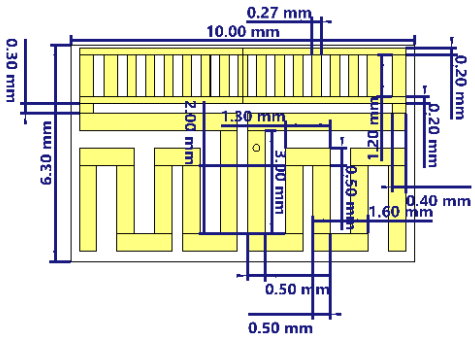

Figure 2. Design of the antenna in CST with dimension

Table 1. Design element in Stage A

Element	Value	Description	Element	Value	Description
LA	0.50 mm	Length	*WA*	1.60 mm	Width
LB	3.00 mm	Length	*WB*	0.50 mm	Width
LC	2.00 mm	Length	*WC*	0.50 mm	Width
LD	0.50 mm	Length	*WD*	1.30 mm	Width
LK	0.30 mm	Length	*WF*	1.30 mm	Width
LL	0.20 mm	Length	*WK*	0.40 mm	Width
LM	1.20 mm	Length	*WO*	0.13 mm	Width
LN	0.20 mm	Length	*WT*	0.27 mm	Width
LO	1.20 mm	Length	*SP*	0.27 mm	Width
LT	1.20 mm	Length	*SUBt*	0.59 mm	Substrate Thickness
ROCore	0.10 mm	Outer Core	*SUB X*	10.00 mm	Substrate Width
RICore	0.00 mm	Inner Core	*SUBY*	6.00 mm	Substrate Length
ROTeflon	RO Hole	Outer Teflon	*ANTt*	0.035 mm	Antenna Thickness
RITeflon	RO Core	Inner Teflon	*GNDt*	0.035 mm	Ground Thickness
ROHole	0.125*2	Outer Hole	*Coax X*	0.80 mm	Probe Width
RICasing	ROTeflon	Inner Casing	*Coax Y*	1.00 mm	Probe Length
ROCasing	ROTeflon +0.035 mm	Outer Casing	*HUp*	*ANTt+ GNDt+ SUBt+* 0.035 mm	Length Feed
HDown	SUBt	Length Teflon	*Hcasing*	1.00 mm	Length Casing

2.2.2 ***Stage B***

Design C is the optimized design of the antenna from Design B to further improve its operation performance in the fat layer. First step on the optimization starts with the *SUBX* and *SUBY* which involve further size reduction of the antenna. The effect of reducing the size of the antenna is not only in the increasing trend of the resonance frequency [7] but it is also good to be implanted inside the human body.

The final design of the antenna the length of the substrate is *SUBX*=4mm and the width of the substrate is *SUBY*=5.08 mm in the initial design of the antenna. The thickness of the ground plane and the radiating patch are *ANTt*=0.035 mm, *GNDTt*=0.035 mm respectively and the patch thickness is *SUBt*=0.59 mm. The illustration depicts the surface view of the proposed antenna together with its geometrical specifications as shown in Figure 3 and Figure 4 with Table 2 design element in Stage B.

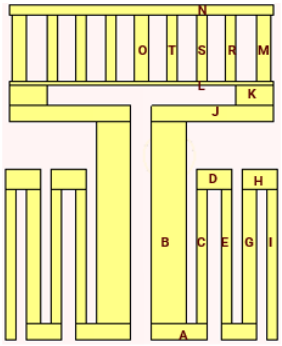

Figure 3. Design B in CST top view

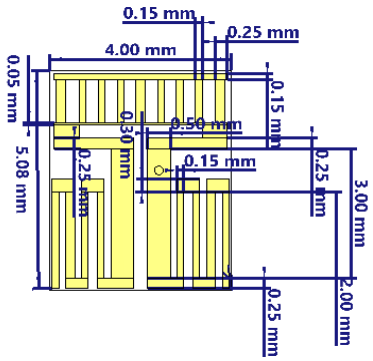

Figure 4. Design of the antenna in CST with dimension

3. RESULTS AND DISCUSSION

3.1.1 Performance Measurements in the fat layer of Human Body Model

S_{11} parameter, also known as the reflection coefficient, shows the power reflected from the antenna toward the source. Figure 4.1 shows the simulated result of the antenna at free space with S11 value -28.92 dB which is an acceptable limit at the operating frequency of 2.4 GHz. The realized gain that obtained from this simulation is -21.81 dBi. In overall, it is observed that the performance of the antenna is good. However, this result is the pre-optimization results of the antenna before it is being simulated inside the human body. After obtaining the good performance of the designed antenna in the free space, design of the antenna B then will be simulated inside the human body layer which is within the fat layer.

The human body was modeled with the average data of the permittivity, conductivities, and thicknesses of each layer extracted from [13-23] as shown in Figure 5 and Table 3. The simulated and measured reflection coefficient, S_{11} is displayed in Figure 6. Design B of the proposed PIFA antenna resonates at frequency 1.15 GHz, 2.84 GHz, and 3.84 GHz with the S11 -31.29 dB, -13.46 dB and -10.91 dB respectively. The results of the reflection loss are still acceptable though it is degrading from one resonance frequency to another as shown in Table 4.

Table 2. Design element in Stage B

Element	Value	Description	Element	Value	Description
LA	0.25 mm	Length	*WA*	0.80 mm	Width
LB	3.00 mm	Length	*WB*	0.50 mm	Width
LC	2.00 mm	Length	*WC*	0.15 mm	Width
LD	0.30 mm	Length	*WD*	0.50 mm	Width
LK	0.30 mm	Length	*WF*	0.50 mm	Width
LL	0.05 mm	Length	*WK*	0.20 mm	Width
LM	1.00 mm	Length	*WO*	0.10 mm	Width
LN	0.15 mm	Length	*WT*	0.15 mm	Width
LO	1.00 mm	Length	*SP*	0.27 mm	Width
LT	1.00 mm	Length	*SUBt*	0.59 mm	Substrate Thickness
ROCore	0.10 mm	Outer Core	*SUBX*	4.00 mm	Substrate Width
RICore	0.00 mm	Inner Core	*SUBY*	5.08 mm	Substrate Length
ROTeflon	*ROHole*	Outer Teflon	*ANTt*	0.035 mm	Antenna Thickness
RITeflon	*ROCore*	Inner Teflon	*GNDt*	0.035 mm	Ground Thickness
ROHole	0.125 *2	Outer Hole	*CoaxX*	0.80 mm	Probe Width
RICasing	*ROTeflon*	Inner Casing	*CoaxY*	1.00 mm	Probe Length
ROCasing	*ROTeflon +0.035 mm*	Outer Casing	*HUp*	*ANTt+ GNDt + SUBt+* 0.035 mm	Length Feed
HDown	*SUBt*	Length Teflon	*Hcasing*	1.00 mm	Length Casing

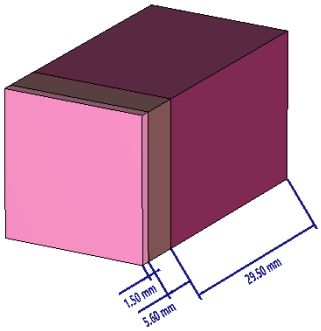

Figure 5. Body model of arm layer

Table 3. Average of thickness, permittivity, and conductivity of arm part

Body Part	Sub Body Part	Thickness (mm)	Permittivity, ε_r	Conductivity, σ
TS	Skin	1.5	32.82	1.34
TF	Fat	5.6	15.32	0.195
TMu	Muscle	29.5	51.27	1.19

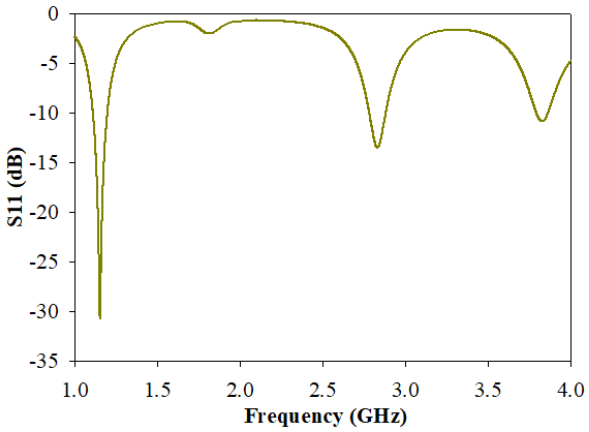

Figure 6. S_{11} within human fat layer

Table 4. Performance of the antenna at different frequency

Frequency Antenna (GHz)	Performance of the antenna at different frequency		
	Return Loss (S_{11})	Gain (dBi)	Total Efficiency (%)
1.15	-31.29 dB	-34.52	-38.22
2.84	-13.46 dB	-23.41	-26.36
3.84	-10.91 dB	-16.62	-18.60

3.1.1 Optimization Inside Fat within the Human Body Model

After obtaining the results from the simulation of the antenna in the human fat layer, the antenna is further optimized as the main objective of this project is to simulate an implantable antenna for optimal performance in the selected fat layer. The results that have been obtained in Design A is not in good performance of the antenna within the human fat layer. The first step that have been taken in optimizing the antenna (Design B) was by reducing the size of the antenna which the element in SUBX (width) and SUBY (length). By reducing the size of SUBX and SUBY elements, WA and LB elements also need to be reduced. Figure 7 shows the design of the antenna at the first step of the optimization.

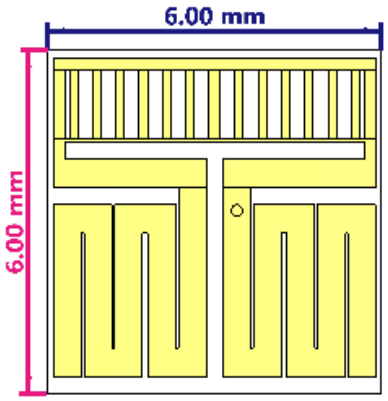

Figure 7. First step of design optimization

Figure 8 shows the results of the S11 at the first stage optimization with the reflection coefficient is -9.56 dB which is not within acceptable limit of S S11 ≤ -10 dB However, the resonant frequency of the antenna is shifted to the right from 1.15 GHz to 2.01 GHz showing that by reducing the size of the antenna will improve its operating frequency towards 2.4 GHz. The shifting towards 2.4 GHz is desirable for operation at the ISM band of 2.4 GHz application. The radiating part of the antenna in meander shape is too close to another other without having sufficient space gap affecting undesirable coupling between them is one of the possibilities that makes the return loss results beyond the acceptable limit. The resonance frequency that has been obtained has yet to operate at the ISM band thus, the size of the antenna needs to be reduced further. Table 5 shows the changed value of the design element from the first step.

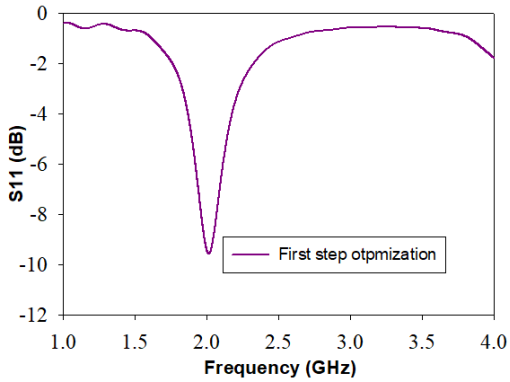

Figure 8. S_{11} results of first step optimization of the antenna

Table 5. Changes value of the design element from the first stage optimization

Element	Initial Value (mm)	New Value (mm)
SUBX	10.00	6.00
SUBY	6.30	6.00
WA	1.06	1.01
LB	3.00	2.70

The second stage optimization of the antenna is focusing on reducing the size of the antenna and the meander shape-element of the antenna that is closer to one another. Figure 9 shows the S_{11} graph based on the parameter sweep analysis of the antenna and Table 6 shows the iteration of the parameter in this step. Figure 10 shows the design of the antenna with element changes from stage two. The best and optimum value was selected for this iteration after obtaining the results of parameter sweep, where it is shown at Figure 9. 3rd Iteration 3 considerable results with changing parameters LL = 0.05 mm, LN = 0.20 mm, LO = 1.00 mm, and SUBY = 5.60 mm as shown in Table 5. However, results at 3rd iteration with the reflection coefficient, S_{11} is -26.66 dB at the 2.21 GHz operating frequency. The return loss is within the acceptable limit, but the operating frequency needs another optimization so that the antenna can be operated in optimal performance in the fat layer.

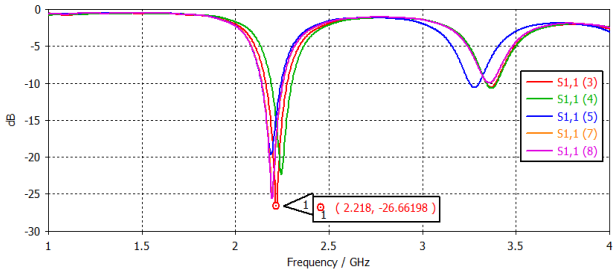

Figure 9. S_{11} graph based on parameter sweep from stage 2

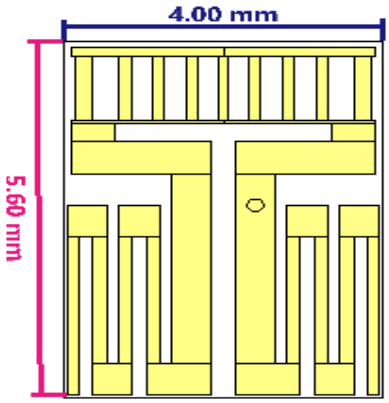

Figure 10. Design of the antenna with the element changes from stage two

Table 6. Parameter iteration of stage two optimization

Parameter iteration				
Iteration	**LL**	**LN**	**LO**	**SUBY**
3rd	0.05	0.20	1.00	5.60
4th	0.10	0.15	1.00	5.60
5th	0.30	0.15	1.00	5.60
7th	0.30	0.15	1.00	5.60
8th	0.05	0.15	0.80	5.60

The best and optimum value was selected after obtaining the results of parameter sweep which is at 10th iteration, where it is demonstrated at Figure 11 and Table 7. Iteration 10 has considerable results with parameter changing LA = 0.25 mm, LB = 3.00 mm, LD = 0.30 mm, and SUBY = 5.08 mm. The best S_{11} slope is at 2.40 GHz operating frequency with Lower Frequency (LF) at 2.34 GHz and Higher Frequency (HF) 2.47 GHz with the results of S_{11} is -43.42 dB which it can be concluded that the best optimal performance of the antenna in human fat layer. Figure 12 demonstrated the final design of the implantable antenna. Figure 13 shows the antenna performance before and after optimization of the antenna. Table 6 shows the summary performance of the antenna after optimization.

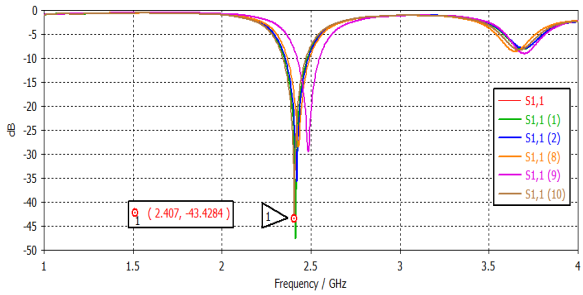

Figure 11. S_{11} graph based on parameter sweep from stage 3

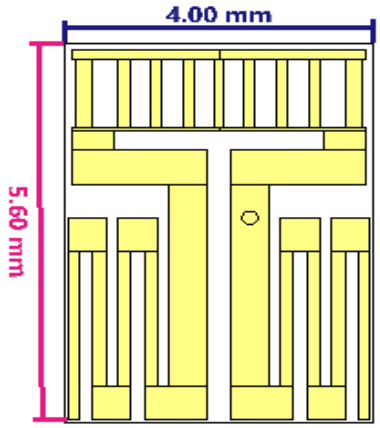

Figure 12. Final design of implantable antenna

Table 7. Parameter iteration stage 3

Parameter iteration				
Iteration	**LA**	**LB**	**LD**	**SUBY**
1st	0.25	3.00	0.25	5.09
2nd	0.25	3.00	0.25	5.07
8th	0.28	2.90	0.35	5.00
9th	0.28	2.80	0.35	4.90
10th	0.25	3.00	0.30	5.08

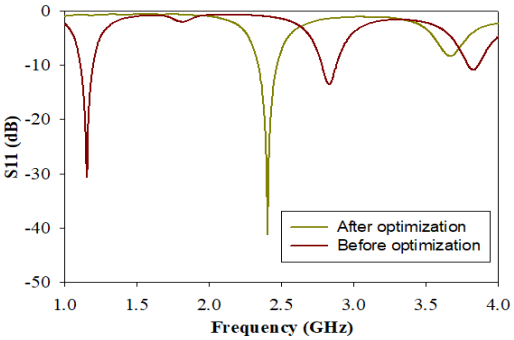

Figure 13. S_{11} comparison before and after optimization.

Table 8 shows the size and gain reduction table of this project compared to previous researchers. The results obtained from the previous work of the implantable

antenna is 74% - 98 % of the size reduction. The realized gain difference from the previous work compared to this project is -0.99 dBi to 5.90 dBi of the realized gain difference. Table 7 shows the size and realized gain comparison of the proposed work with previous research. The proposed work successfully reduced the size of the implantable antenna by 74 to 98% while simultaneously achieve a better realized gain of maximum 5.9 dBI.

Table 8. Size comparison and realized gain difference of the proposed antenna

Ref	Volume (mm^3)	Permittivity of Substrate, εr	Size in λ_r (mm^3)	Size Reduction (%)	Realized Gain (dBi)	Realized Gain (dBi) difference
[8]	19.60 × 19.60 × 1.00	3.10	1.53×10^{-12}	-96.00	-23.00	5.90
[9]	8.00 × 6.00 × 1.00	3.60	2.37×10^{-12}	-74.00	-17.01	-0.99
[10]	19.00 × 19.40 × 1.27	10.20	1.55×10^{-12}	-97.41	-22.00	4.00
[11]	13.50 × 19.50 × 1.905	10.20	1.53×10^{-12}	-97.59	-23.20	5.20
Proposed	4.00 × 5.13 × 0.66	10.80	1.51×10^{-12}		-18.00	-

4. CONCLUSION

In conclusion, the antenna is successfully designed and optimized. The designed antenna was simulated in fat layer of the human body which the initial performance of the antenna was degraded. The optimization of the antenna was done to obtain the optimal performance of the antenna within human fat layer. the PIFA biocompatible implantable antenna successfully operates at the frequency of 2.4GHz (ISM band) application following optimization performance of the antenna within fat layer. This study of a biocompatible implantable antenna showed that the performance of the antenna is affected based on the human tissue layer properties and transient movement of the antenna within the tissue layer (skin, fat and muscle). The developed antenna satisfies all requirements for an implantable antenna, such small size, biocompatibility, low return loss, and acceptable performance in fat layer

ACKNOWLEDGMENT

The authors would like to thank the Ministry of Higher Education (MOHE), School of Postgraduate Studies (SPS), Research Management Centre, Advanced Diagnostics and Progressive Human Care Research Group, Faculty of Electrical Engineering and Universiti Teknologi Malaysia (UTM), Johor Bahru, for the support of the research under UTM Encouragement Research Grant Q.J130000.3851.20J74

REFERENCES

[1] M. K. Magill, G. A. Conway, and W. G. Scanlon, "Tissue-Independent Implantable Antenna for In-Body Communications at 2.36-2.5 GHz," *IEEE Transactions on Antennas and Propagation*, vol. 65, no. 9, pp. 4406–4417, Sep. 2017, doi: 10.1109/TAP.2017.2708119.

[2] I. J. O. Electromagnetics and A. Microwaves, "Dual-Band Skin-Adhesive Repeater Antenna for Continuous Body Signals Monitoring," *MEDICINE AND BIOLOGY*, vol. 2, no. 1, p. 25, 2018, doi: 10.1109/JERM.2018.2806186.

[3] T. Khajawal, Q. Rubani, A. Rajawat, and S. H. Gupta, "Performance analysis and optimization of band gap of terahertz antenna for WBAN applications," *Optik (Stuttg)*, vol. 243, p. 167387, Oct. 2021, doi: 10.1016/J.IJLEO.2021.167387

[4] M. M. Soliman et al., "Review on medical implantable antenna technology and imminent research challenges," Sensors, vol. 21, no. 9. MDPI AG, May 01, 2021. doi: 10.3390/s21093163.

[5] A. Ibraheem and M. Manteghi, "Performance of an implanted electrically coupled loop antenna inside human body," Progress in Electromagnetics Research, vol. 145, pp. 195–202, 2014, doi: 10.2528/PIER14022005.

[6] C. Liu, Y. Zhang, and X. Liu, "Circularly Polarized Implantable Antenna for 915 MHz ISM-Band Far-Field Wireless Power Transmission; Circularly Polarized Implantable Antenna for 915 MHz ISM-Band Far-Field Wireless Power Transmission," IEEE ANTENNAS AND WIRELESS PROPAGATION LETTERS, vol. 17, no. 3, p. 373, 2018, doi: 10.1109/LAWP.2018.2790418.

[7] R. K. Mahesh and B. Suryakanth, "A Study of Planar Inverted F Antenna (PIFA) for Wireless Applications," *International Journal on Emerging Technologies (Special Issue on NCRIET-2015)*, vol. 6, no. 2, pp. 193–196, 2015, [Online]. Available: www.researchtrend.net

[8] S. M. Huang, M. R. Tofighi, and A. Rosen, "Considerations for the Design and Placement of Implantable Annular Slot Antennas for Intracranial Pressure Monitoring Devices," *IEEE Antennas and Wireless Propagation Letters*, vol. 14, pp. 1514–1517, 2015, doi: 10.1109/LAWP.2014.2370940.

[9] M. Mohiuddin Miran and F. Arifin, *Design and Performance Analysis of a Miniaturized Implantable PIFA for Wireless Body Area Network Applications; Design and Performance Analysis of a Miniaturized Implantable PIFA for Wireless Body Area Network Applications*. 2019.

[10] L. J. Xu, Y. X. Guo, and W. Wu, "Dual-band implantable antenna with open-end slots on ground," IEEE Antennas and Wireless Propagation Letters, vol. 11, pp. 1564–1567, 2012, doi: 10.1109/LAWP.2012.2237010.*IEEE Criteria for Class IE Electric Systems* (Standards style), IEEE Standard 308, 1969.

[11] X. T. Yang, H. Wong, and J. Xiang, "Polarization reconfigurable planar inverted-F antenna for implantable telemetry applications," IEEE Access, vol. 7, pp. 141900–141909, 2019, doi: 10.1109/ACCESS.2019.2941388.

[12] G. A. Casula and G. Montisci, "A Design Rule to Reduce the Human Body Effect on Wearable PIFA Antennas," *Electronics (Switzerland)*, vol. 8, no. 2, pp. 1-18, 2019, doi: 10.3390/electronics8020244.

[13] H. K. Nie, X. W. Xuan, and G. J. Ren, "Wearable antenna pressure sensor with electromagnetic bandgap for elderly fall monitoring," *AEU - International Journal of Electronics and Communications*, vol. 138, p. 153861, 2021, doi: 10.1016/J.AEUE.2021.153861.

[14] W. el May, I. Sfar, J. M. Ribero, and L. Osman, "Design of Low-Profile and Safe Low SAR Tri-Band Textile EBG-Based Antenna for IoT Applications" *Progress in Electromagnetics Research Letters,* vol. 98, pp. 85-94, 2021, doi:10.2528/PIERL21051107

[15] U. Ali, S. Ullah, J. Khan, M. Shafi, B. Kamal, A. Basir and R. D. Seager, "Design and SAR analysis of wearable antenna on various parts of human body, using conventional and artificial ground planes," Journal of Electrical Engineering and Technology, vol. 12, no. 1, pp. 317–328, 2017, doi: 10.5370/JEET.2017.12.1.317.

[16] S. Das and D. Mitra, "A Compact Wideband Flexible Implantable Slot Antenna Design with Enhanced Gain," in IEEE Transactions on Antennas and Propagation, vol. 66, no. 8, pp. 4309-4314, 2018, doi: 10.1109/TAP.2018.2836463

[17] Y. Gmih and A. Farchi, "Compact Antenna for UHF-RFID Tag Tested on Human Body for Identification Cards," *International Journal of Intelligent Engineering and Systems*, vol. 13, no. 1, pp. 1–10, 2020, doi: 10.22266/IJIES2020.0229.21.

[18] G. L. Huang, C. Y. D. Sim, S. Y. Liang, W. S. Liao, and T. Yuan, "Low-Profile Flexible UHF RFID Tag Design for Wristbands Applications," Hindawi, pp. 1-4, 2018, doi: 10.1155/2018/9482919.

[19] D. Marques, M. Egels, and P. Pannier, "Broadband UHF RFID Tag Antenna for Bio-Monitoring," *Progress in Electromagnetics Research B,* vol. 67, pp. 31-44, 2016, doi:10.2528/PIERB16020103

[20] I. Bouhassoune, H. Chaibi, A. Chehri and R. Saadane "UHF RFID Spiral-Loaded Dipole Tag Antenna Conception for Healthcare Applications," *Science Direct*, vol. 192, pp. 2531-2539, 2021, doi : 10.1016/j.procs.2021.09.022

[21] S. Amendola, S. Milici and G. Marrocco, "Performance of Epidermal RFID Dual-loop Tag and On-Skin Retuning," in IEEE Transactions on Antennas and Propagation, vol. 63, no. 8, pp. 3672-3680, 2015, doi: 10.1109/TAP.2015.2441211.

[22] F. Amato, C. Occhiuzzi, and G. Marrocco, "Epidermal Backscattering Antennas in the 5G Framework: Performance and Perspectives," IEEE Journal of Radio Frequency Identification, vol. 4, no. 3, pp. 176–185, 2020, doi: 10.1109/JRFID.2020.2998082.

[23] A. Y. I. Ashyap, S. H. B. Dahlan, Z. Z. Abidin, M. H. Dahri, H. A. Majid, M. R. Kamarudin, S. K. Yee, M. H. Jamaludin, A. Alomainy and Q. H. Abbasi "Robust and Efficient Integrated Antenna With EBG-DGS Enabled Wide Bandwidth for Wearable Medical Device Applications" *IEEE Access*, vol. 8, pp. 56346-56358, 2020, doi: 10.1109/ACCESS.2020.2981867.